JOURNAL OF SOLID STATE CHEMISTRY 43, 190–195 (1982)

# $Nd^{3+}$, $Eu^{3+}$, and $Gd^{3+}$ Ions as Local Probes in the $Na_xSr_{3-2x}Ln_x(PO_4)_2$ and $KCaLn(PO_4)_2$ Rare Earth Phosphates

C. PARENT, P. BOCHU, A. DAOUDI,* AND G. LE FLEM

*Laboratoire de Chimie du Solide du CNRS, 351, cours de la Libération, 33405 Talence Cedex, France*

Received December 16, 1981; in final form March 2, 1982

Use of $Nd^{3+}$, $Eu^{3+}$, and $Gd^{3+}$ as local structural probes allows the determination of the rare earth positions in the $Na_xSr_{3-2x}Ln_x(PO_4)_2$ ($Ln$ = La to Tb) and $KCaLn(PO_4)_2$ phases ($Ln$ = rare earth). Moreover, a common feature of both series is a particularly high splitting of the excitation $^6P_{7/2}$ and $^6P_{5/2}$ levels of the $Gd^{3+}$ ions.

In a previous structural study the $Na_xSr_{3-2x}Ln_x(PO_4)_2$ (*1*) and $KCaLn(PO_4)_2$ (*2*) phases have been assumed to be isotypic, respectively, with $Sr_3(PO_4)_2$ (*3*) and the hexagonal variety of $CePO_4$.

In order to determine the cationic distribution in the lattices an optical study using $Nd^{3+}$, $Eu^{3+}$, or $Gd^{3+}$ ion probes was carried out. The activator concentrations were chosen to allow a good emission intensity.

## I. Preparation of the Materials

The powder samples were prepared from stoichiometric mixtures of alkali or alkaline-earth carbonates (99.5%), rare earth oxides (Rhône-Poulenc 99.99%), and diammonium hydrogenophosphate (Merck min. 99%).

Single crystals of $KCaNd(PO_4)_2$ were grown by recrystallization of the powder at 1600°C in a sealed platinum tube followed by slow cooling.

* Present address: Faculté des Sciences, Université Mohammed V, avenue Ibn Batouta, Rabat, Morocco.

## II. The $Na_xSr_{3-2x}Ln_x(PO_4)_2$ Phases ($Ln$ = La to Tb)

The $Sr_3(PO_4)_2$ structure involves two types of strontium sites (Fig. 1):

—a $Sr_I$ C.N. XII site with inversion symmetry ($D_{3d}$), in which $\langle Sr-O\rangle \simeq 2.87$ Å.

—a $Sr_{II}$ C.N. X site without inversion symmetry ($C_{3v}$), in which $\langle Sr-O\rangle \simeq 2.67$ Å.

The investigated $Na_xSr_{3-2x}Ln_x(PO_4)_2$ phases have a $Sr_3(PO_4)_2$-type structure due to coupled substitution:

$$2\,Sr^{2+} = Ln^{3+} + Na^+ \qquad (Ln = \text{La to Tb}). \quad (1)$$

The $Ln^{3+}$ ions may fill either $Sr_I$ or $Sr_{II}$ sites. A study of the luminescent properties of $Na_{0.20}Sr_{2.60}Eu_{0.20}(PO_4)_2$ and $Na_{0.55}Sr_{1.90}Gd_{0.55}(PO_4)_2$ has allowed us to determine the cationic distribution.

The coupled substitution induces only cell-parameter variations below or equal to 1%, and the $Ln-O$ distances were assumed to be equal to the Sr–O distances in $Sr_3(PO_4)_2$ (*3*).

0022-4596/82/080190-06$02.00/0

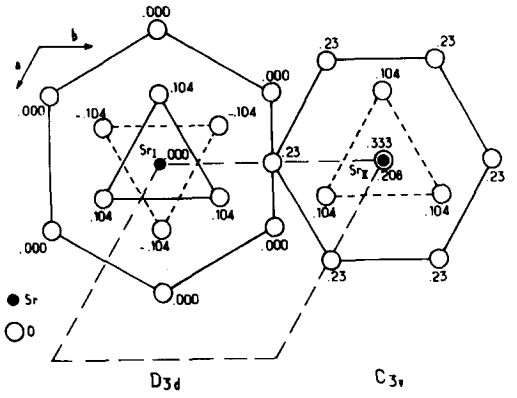


FIG. 1. $Sr_I$ and $Sr_{II}$ sites in the $Sr_3(PO_4)_2$ lattice.

### *II.1.* $^5D_0 \rightarrow {}^7F_J$ ($J = 0,1,2$) *Emission of* $Eu^{3+}$ *in* $Na_{0.20}Sr_{2.60}Eu_{0.20}(PO_4)_2$

The $^5D_0 \rightarrow {}^7F_J$ ($J = 0,1,2$) emission spectrum of $Eu^{3+}$ in $Na_{0.20}Sr_{2.60}Eu_{0.20}(PO_4)_2$ recorded at 80K under 380-nm excitation is given in Fig. 2.

It consists of one line for the $^5D_0 \rightarrow {}^7F_0$ transition, two lines for $^5D_0 \rightarrow {}^7F_1$, and three lines for $^5D_0 \rightarrow {}^7F_2$ (Table I).

This result illustrates the occupancy of only one site without inversion symmetry and with a hexagonal or trigonal point symmetry, i.e., the $C_{3v}$ $Sr_{II}$ position in the $Sr_3(PO_4)_2$ network.

The energy corresponding to the $^5D_0 \rightarrow {}^7F_0$ emission (17,316 $cm^{-1}$) is of the same order of magnitude as those observed for $SrTiO_3:Eu^{3+}$ (17,034 $cm^{-1}$) or $Sr_2TiO_4:Eu^{3+}$ (17.340 $cm^{-1}$) (5), in which ⟨Eu–O⟩ distances are, respectively, 2.76 and 2.72 Å.

TABLE I

$^5D_0 \rightarrow {}^7F_J$ ($J = 0,1,2$) EMISSION LINES OF $Eu^{3+}$ IN $Na_{0.20}Sr_{2.60}Eu_{0.20}(PO_4)_2$ UNDER 380-nm EXCITATION ($T = 80K$)

| $Na_{0.20}Sr_{2.60}Eu_{0.20}(PO_4)_2$ | λ (nm) | $E$ ($cm^{-1}$) |
|---|---|---|
| $^5D_0 \rightarrow {}^7F_0$ | 577.5 | 17,316 |
| $^5D_0 \rightarrow {}^7F_1$ | 586.5 | 17,050 |
| | 598.9 | 16,697 |
| $^5D_0 \rightarrow {}^7F_2$ | 609.6 | 16,404 |
| | 612.3 | 16,332 |
| | 616.2 | 16,228 |

TABLE II

WAVELENGTHS AND ENERGIES OF THE $^6P_{7/2} \rightarrow {}^8S_{7/2}$ TRANSITIONS OF $Gd^{3+}$ IN $Na_{0.55}Sr_{1.90}Gd_{0.55}(PO_4)_2$ ($T = 80$ AND 300K)

| | $^6P_{7/2} \rightarrow {}^8S_{7/2}$ | |
|---|---|---|
| $Na_{0.55}Sr_{1.90}Gd_{0.55}(PO_4)_2$ | λ(nm) | $E$($cm^{-1}$) |
| $T = 300K$ | 310.89 | 32,166 |
| | 311.20 | 32,134 |
| | 311.86 | 32,066 |
| | 312.91 | 31,958 |
| $T = 80K$ | 310.98 | 32,156 |
| | 311.37 | 32,116 |
| | 311.97 | 32,054 |
| | 313.05 | 31,944 |

### *II.2 Optical Properties of* $Na_{0.55}Sr_{1.90}Gd_{0.55}(PO_4)_2$

The $^6P_{7/2} \rightarrow {}^8S_{7/2}$ emission was studied at 80 and 300K under 273-nm excitation (Fig. 3, Table II).

Whatever the recording temperature the emission spectrum is constituted by four

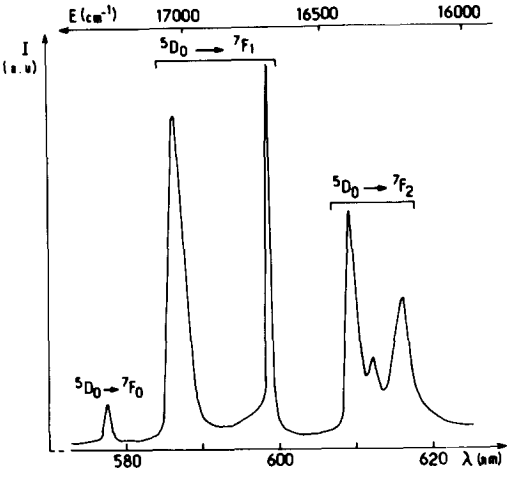


FIG. 2. Emission spectrum of $Eu^{3+}$ in $Na_{0.20}Sr_{2.60}Eu_{0.20}(PO_4)_2$ under 380-nm excitation ($T = 80K$).

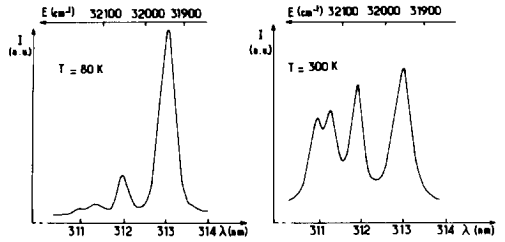


FIG. 3. $^6P_{7/2} \rightarrow {}^8S_{7/2}$ emission spectra of $Gd^{3+}$ in $Na_{0.55}Sr_{1.90}Gd_{0.55}(PO_4)_2$ under 273-nm excitation. ($T$ = 80 and 300K).

lines whose intensities are in good agreement with a Boltzmann distribution.

The excitation spectrum corresponding to this emission recorded at 80K is given in Fig. 4. The obtained wavelengths and energies are listed in Table III. No variation of this spectrum was observed by changing the emission wavelength. It consists of three lines for the $^8S_{7/2} \rightarrow {}^2P_{5/2}$ transition and two lines for $^8S_{7/2} \rightarrow {}^2P_{3/2}$.

Such an emission spectrum and, mainly, the presence of the dipolar electric $^8S_{7/2} \rightarrow {}^2P_{3/2}$ transition confirm the occupancy by $Gd^{3+}$ ions of only one type of site, the $Sr_{II}$ site, without inversion symmetry.

The barycenters of the $^6P_{7/2}$ and $^6P_{5/2}$ levels at 80K are found at high energies (respectively, 32,102 and 32,655 $cm^{-1}$) typical of a large ⟨Gd–O⟩ distance, i.e., here about 2.67 Å (*6*, *7*).

The crystal-field splitting for both levels,

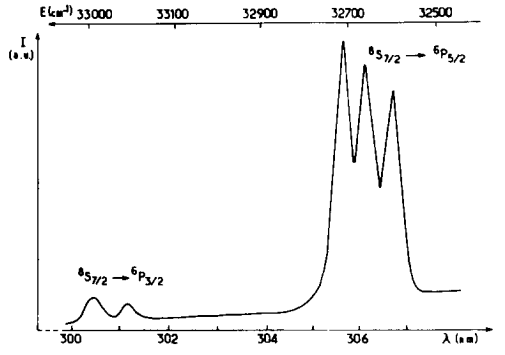


FIG. 4. Excitation spectrum of the $^6P_{7/2} \rightarrow {}^8S_{7/2}$ emission of $Gd^{3+}$ in $Na_{0.55}Sr_{1.90}Gd_{0.55}(PO_4)_2$ ($T$ = 80 K).

TABLE III

EXCITATION LINES OF THE $Gd^{3+}$ $^6P_{7/2} \rightarrow {}^8S_{7/2}$ EMISSION IN $Na_{0.55}Sr_{1.90}Gd_{0.55}(PO_4)_2$ ($T$ = 80K)

| $Na_{0.55}Sr_{1.90}Gd_{0.55}(PO_4)_2$ | λ (nm) | $E$ ($cm^{-1}$) |
|---|---|---|
| $^8S_{7/2} \rightarrow {}^6P_{3/2}$ | 300.5 | 33,278 |
| | 301.1 | 33,212 |
| $^8S_{7/2} \rightarrow {}^6P_{5/2}$ | 305.7 | 32,712 |
| | 306.2 | 32,658 |
| | 306.8 | 32,594 |

212 $cm^{-1}$ for $^6P_{7/2}$ and 118 $cm^{-1}$ for $^6P_{5/2}$, is rather large for a C.N. X site (*7*). This effect is likely due to the strong anisotropy of the $Sr_{II}$ site which involves in $Sr_3(PO_4)_2$ a short Sr–O distance (2.48 Å), three longer (2.62 Å), and six quite longer lengths (2.72 Å).

## III. The KCa*Ln*$(PO_4)_2$ Phases (*Ln* = Rare Earth)

The *Ln*$PO_4$ (*Ln* = La, Ce, Nd) phosphates crystallize with two allotropic varieties. One has the monazite-type structure with monoclinic symmetry, the other one has a hexagonal symmetry. In this last structure, a three-dimensional covalent network is made up of $(PO_4)$ groups and $(LnO_8)$ polyhedra sharing edges or corners. The point symmetry of the rare earth site is $D_2$ with ⟨Ln–O⟩ = 2.40 Å (Fig. 5). The structure is characterized by the existence

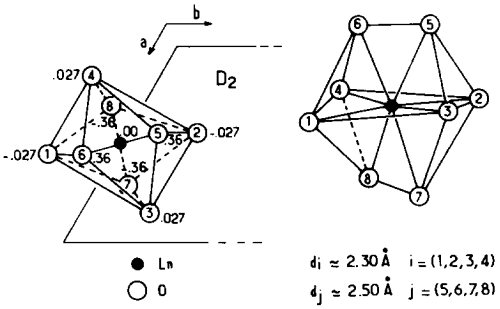


FIG. 5. Rare earth coordination polyhedron in the hexagonal *Ln*$PO_4$ orthophosphates (*Ln* = La, Ce, Nd).

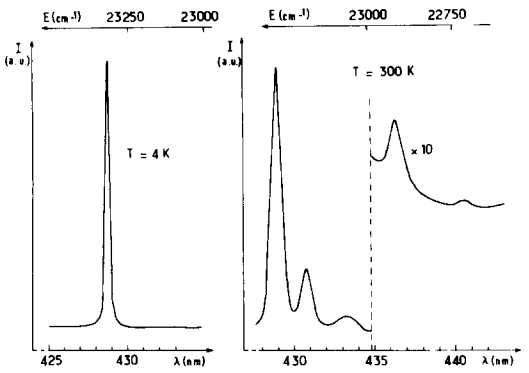


FIG. 6. $^4I_{9/2} \rightarrow {}^2P_{1/2}$ absorption spectra of $Nd^3$ in $KCaNd(PO_4)_2$ at 4 and 300K.

of large tunnels running along the c axis and able to contain zeolitic water.

New isotypical phases with general formula $ACaLn(PO_4)_2$ ($A$ = K, Rb, Cs; $Ln$ = rare earth) have been prepared by introducing $A^+$ ions in these tunnels and $Ca^{2+}$ ions in half of the rare earth sites (*2*).

To confirm this hypothesis of cationic distribution the luminescence of three of these orthophosphates, $KCaNd(PO_4)_2$, $KCaEu(PO_4)_2$, and $KCaGd(PO_4)_2$ was studied.

### *III.1.* $^4I_{9/2} \rightarrow {}^2P_{1/2}$ *Absorption of* $Nd^{3+}$ *in* $KCaNd(PO_4)_2$

The $^4I_{9/2} \rightarrow {}^2P_{1/2}$ absorption of $Nd^{3+}$ in single crystals of $KCaNd(PO_4)_2$ was studied at 4 and 300K (Fig. 6, Table IV).

The number of absorption lines (one at 4K, five at 300K) is a proof of the presence of $Nd^{3+}$ in one type of site only.

TABLE IV

$^4I_{9/2} \rightarrow {}^2P_{1/2}$ ABSORPTION OF $Nd^{3+}$ IN $KCaNd(PO_4)_2$ ($T$ = 4 AND 300K)

| | $^4I_{9/2} \rightarrow {}^2P_{1/2}$ | |
|---|---|---|
| $KCaNd(PO_4)_2$ | λ(nm) | $E$(cm$^{-1}$) |
| $T$ = 4K | 428.6 | 23,332 |
| | 428.8 | 23,321 |
| | 430.7 | 23,218 |
| $T$ = 300K | 433.3 | 23,079 |
| | 436.4 | 22,915 |
| | 440.7 | 22,691 |

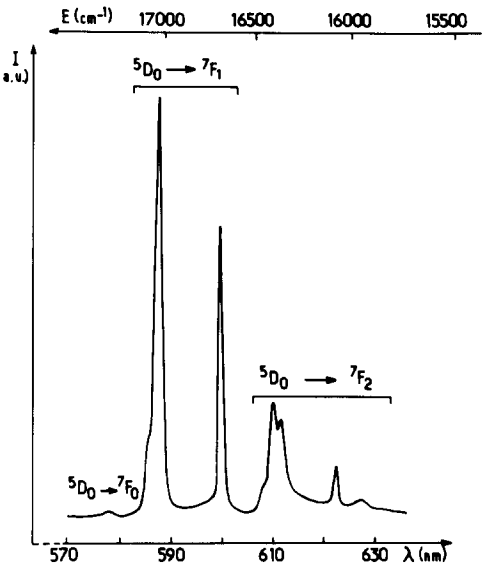


FIG. 7. Emission spectrum of $Eu^{3+}$ in $KCaEu(PO_4)_2$ under 380-nm excitation ($T$ = 80K).

The most intense $^4I_{9/2} \rightarrow {}^2P_{1/2}$ line at 300K which corresponds to the lowest $^4I_{9/2}$ Stark level is located at 23,321 cm$^{-1}$. This value is close to that observed for the orthophosphate $Na_3Nd(PO_4)_2$ (23,225 cm$^{-1}$) in which neodymium is in very similar eight- and nine-coordinated sites with a ⟨Nd–O⟩ distance of about 2.50 Å (*8*).

### *III.2.* $^5D_0 \rightarrow {}^7F_J$ ($J$ = 0,1,2) *Emission of* $Eu^{3+}$ *in* $KCaEu(PO_4)_2$

The $^5D_0 \rightarrow {}^7F_J$ ($J$ = 0,1,2) emission was studied at 80K under 380-nm excitation (Fig. 7, Table V).

The number of the observed lines (one for $^5D_0 \rightarrow {}^7F_0$, three for $^5D_0 \rightarrow {}^7F_1$, and five for $^5D_0 \rightarrow {}^7F_2$) confirms the unicity of the rare earth site and may be in accordance with a $D_2$ symmetry.

The value of the $^5D_0 \rightarrow {}^7F_0$ transition energy is higher than the typical value for $Eu^{3+}$ ions in a C.N. VIII site with ⟨Eu–O⟩ = 2.40 Å (*5*). According to Caro *et al.* such a behavior could be the consequence of par-

TABLE V

$^5D_0 \rightarrow {}^7F_J$ ($J$ = 0,1,2) EMISSION OF $Eu^{3+}$ IN $KCaEu(PO_4)_2$ UNDER 380-nm EXCITATION ($T$ = 80K)

| $KCaEu(PO_4)_2$ | λ (nm) | $E$ ($cm^{-1}$) |
|---|---|---|
| $^5D_0 \rightarrow {}^7F_0$ | 578.0 | 17,301 |
| | 587.2 | 17,030 |
| $^5D_0 \rightarrow {}^7F_1$ | 588.0 | 17,007 |
| | 600.0 | 16,667 |
| | 609.2 | 16,415 |
| | 610.4 | 16,383 |
| $^5D_0 \rightarrow {}^7F_2$ | 612.0 | 16,340 |
| | 622.5 | 16,064 |
| | 627.0 | 15,949 |

ticularly weak values of the $E_2$ and $E_3$ Racah parameters which are related to specific arrangements of the ligands around the $Eu^{3+}$ ion (*5*, *9*). As a matter of fact two different groups of $Ln$–O distances exist in the $D_2$ site (Fig. 5).

### *III.3. Optical Properties of the $KCaGd(PO_4)_2$ Phase*

Figure 8 gives the $^6P_{7/2} \rightarrow {}^8S_{7/2}$ emission spectra of $Gd^{3+}$ in $KCaGd(PO_4)_2$ recorded at 80 and 300K under 274-nm excitation. The corresponding excitation spectrum of this emission is given in Fig. 9. The obtained wavelengths and energies are listed in Tables VI and VII.

These results can be usefully compared with those relative to $Na_{0.55}Sr_{1.90}Gd_{0.55}$

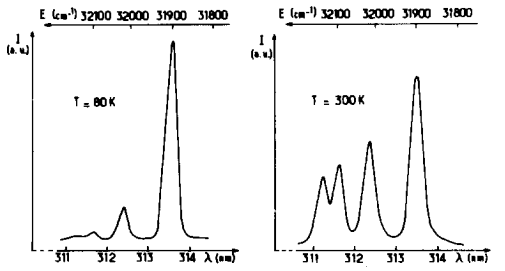


FIG. 8. $^6P_{7/2} \rightarrow {}^8S_{7/2}$ emission spectra of $Gd^{3+}$ in $KCaGd(PO_4)_2$ under 274-nm excitation ($T$ = 80 and 300K).

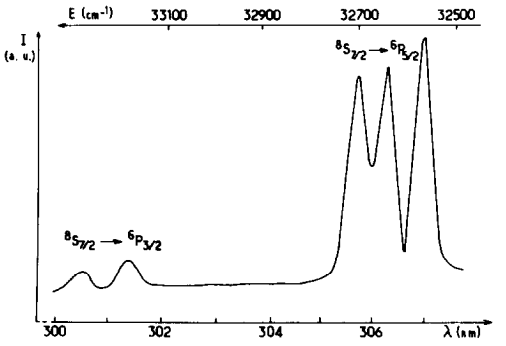


FIG. 9. Excitation spectrum of the $^6P_{7/2} \rightarrow {}^8S_{7/2}$ emission of $Gd^{3+}$ in $KCaGd(PO_4)_2$ ($T$ = 80K).

$(PO_4)_2$: gadolinium ions are located in one site only, without inversion symmetry.

Lowering of the $^6P_{7/2}$ and $^6P_{5/2}$ barycenters at 80K (found here at 32,033 and 32,643 $cm^{-1}$) compared to the previous ones is consistent with decreasing ⟨Gd–O⟩ distance (from 2.67 to 2.40 Å). The positions of these $^6P_{7/2}$ and $^6P_{5/2}$ barycenters are very close to those observed for the Gd(1) site of $Gd_2(M_0O_4)_3$: 32,015 and 32,068 $cm^{-1}$. In this site the gadolinium ions are sevenfold coordinated with ⟨Gd–O⟩ = 2.36 Å (*10*).

Splitting of the $^6P_{7/2}$ and $^6P_{5/2}$ levels is very high, 227 and 138 $cm^{-1}$, respectively. These values can be compared with those observed in $Gd_2(M_0O_4)_3$: 107 and 85 $cm^{-1}$.

TABLE VI

WAVELENGTHS AND ENERGIES OF THE $^6P_{7/2} \rightarrow {}^8S_{7/2}$ TRANSITIONS OF $Gd^{3+}$ IN $KCaGd(PO_4)_2$ ($T$ = 80 AND 300K)

| | $^6P_{7/2} \rightarrow {}^8S_{7/2}$ | |
|---|---|---|
| $KCaGd(PO_4)_2$ | λ(nm) | $E$($cm^{-1}$) |
| $T$ = 300K | 311.26 | 32,127 |
| | 311.65 | 32,087 |
| | 312.35 | 32,015 |
| | 313.46 | 31,902 |
| $T$ = 80K | 311.26 | 32,127 |
| | 311.65 | 32,087 |
| | 312.36 | 32,014 |
| | 313.48 | 31,900 |

TABLE VII

EXCITATION LINES OF THE $Gd^{3+}$ $^6P_{7/2} \rightarrow {}^8S_{7/2}$ EMISSION IN $KCaGd(PO_4)_2$ ($T$ = 80K)

| $KCaGd(PO_4)_2$ | λ (nm) | $E$ ($cm^{-1}$) |
|---|---|---|
| $^8S_{7/2} \rightarrow {}^6P_{3/2}$ | 300.6 | 33,267 |
| | 301.4 | 33,179 |
| $^8S_{7/2} \rightarrow {}^6P_{5/2}$ | 305.8 | 32,701 |
| | 306.4 | 32,637 |
| | 307.1 | 32,563 |

This so far unexplained behavior is likely due to the particular shape of the coordination polyhedron of gadolinium.

## IV. Conclusions

The use of $Eu^{3+}$ and $Gd^{3+}$ as local probes has allowed us to determine the rare earth position in the $Na_xSr_{3-2x}Ln_x(PO_4)_2$ and $KCaLn(PO_4)_2$ phases.

In the first structural type the rare earth ions are located only in the smallest of both available sites, with a ten-fold coordination.

In the second type $Ln^{3+}$ occupies, as expected, a C.N. VIII site.

For the gadolinium compounds, a particularly high splitting of the $^6P_{7/2}$ and $^6P_{5/2}$ excitation levels is observed. A structural justification will be proposed in the near future.

## References


1. C. PARENT, G. LE FLEM, M. ET-TABIROU, AND A. DAOUDI, *Solid State Commun.* **37,** 857 (1981).
2. M. VLASSE, P. BOCHU, C. PARENT, J. P. CHAMINADE, A. DAOUDI, G. LE FLEM, AND P. HAGENMULLER, *Acta Crystallogr. Sect. B,* to be published.
3. W. H. ZACHARIASEN, *Acta Crystallogr.* **1,** 263 (1948).
4. J. DEXPERT-CHYS. Thèse de Doctorat ès-Sciences Physiques, Univ. de Paris XI-Orsay, Paris (1979).
5. P. CARO, O. BEAURY, AND E. ANTIC, *J. Phys.* **37,** 671 (1976).
6. R. D. SHANNON AND C. T. PREWITT, *Acta Crystallogr. Sect. B* **25,** 952 (1969).
7. P. E. CARO, E. ANTIC, L. BEAURY, O. BEAURY, J. DEROUET, M. FAUCHER, C. GUTTER, O. K. MOUNE, AND P. PORCHER, "Spectroscopie des Eléments de Transition et des Eléments Lourds dans les Solides," Colloque CNRS, Lyon (1976).
8. C. PARENT, C. FOUASSIER, AND G. LE FLEM, *J. Electrochem. Soc.* **127,** 2049 (1980).
9. J. DEXPERT-GHYS, M. FAUCHER, AND P. CARO, *J. Solid State Chem.* **19,** 193 (1976).
10. C. GUTTEL, E. ANTIC, AND P. E. CARO, *Phys. Status Solidi B* **81,** 463 (1977).